1994-02

Comparison between Liouville's theorem and observed latitudinal distribution of trapped ions in the plasmapause region

Olsen, R.C.

JOURNAL OF GEOPHYSICAL RESEARCH, VOL. 99, PAGES 2191-2203, FEBRUARY 1, 1994

Comparison Between Liouville's Theorem And Observed Latitudinal Distribution Of Trapped Ions In The Plasmapause Region

R. C. Olsen and L. J. Scott
Department of Physics, Naval Postgraduate School, Monterey, California
S. A. Boardsen
Space Sciences Laboratory, NASA/MSFC, Huntsville, Alabama

Abstract. The presence of anisotropic plasma distributions, trapped at the Earth's magnetic equator, has consequences for the electric field structure which must exist in equilibrium along the magnetic field line. Data from SCATHA and Dynamics Explorer 1indicated that the core ion distributions at the magnetic equator can be well described as bi-Maxwellian distributions, with a perpendicular temperature an order of magnitude larger than the parallel temperature. A collisionless model is developed for the variation in plasma parameters, following the forms developed by Whipple (1977). If the core electron anisotropy is low, the resulting electric field of ~0.1 $\mu V\ m^{-1}$ is pointed away from the equator. Under these conditions the self-consistent electric field will not overcome the effects of magnetic trapping. The resulting potential distribution results in a local maximum in total plasma density at the equator. Only when the electron distribution is primarily field-aligned can there be a density minimum at the equator. Comparisons are made between this model and the observed variations in DE 1 plasma parameters with latitude.

INTRODUCTION

Plasma observations near the earth's magnetic equator in the outer plasmasphere indicate the presence of core plasma distributions that are often highly anisotropic. The core ion distributions are often "pancake" like, that is, with enhanced fluxes at 90° pitch angle. These distributions can be modeled with reasonable success as bi-Maxwellian distributions, with perpendicular temperatures as much as an order of magnitude greater than the parallel temperatures [*Olsen*, 1981].

The anisotropy of the electron distributions will, in general, differ from that found in the ions. In equilibrium, this immediately leads to a requirement for a parallel electric field to maintain charge neutrality [*Alfven and Falthammer*, 1963; *Persson*, 1963; 1966]. The purpose of this paper is to investigate the nature of the electric field that is implied by the equatorial measurements of the SCATHA and Dynamics Explorer 1 satellites near the plasmapause, and the consequences of this electric field for the evolution of the plasma distribution along the field line. The variations in density and perpendicular temperature predicted by kinetic theory will be compared to observations.

OBSERVATIONS OF TRAPPED DISTRIBUTIONS

Previous Reports

Trapped ion (and electron) distributions have been reported for a number of years from the outer plasmasphere, particularly near geosynchronous orbit. Here, the phrase trapped is generally used to mean equatorially trapped, as opposed to field-aligned or isotropic distributions, recognizing that very little of the data described or shown here is associated with questions of trapped vs. loss-cone distributions. Such pitch angle distributions are also typically termed "pancake" distributions.

Ion measurements are relatively more numerous than electron measurements, e.g., *Horwitz and Chappell* [1979], *Comfort and Horwitz* [1981], and *Horwitz et al* [1981]. The work by Horwitz showed that pancake distributions were common near the plasmapause, particularly on the dayside. The ISEE 1 survey did not reach the afternoon/dusk region [*Horwitz et al*, 1981]. GEOS-2 data showed observations of pancake distributions of electrons. These distributions were observed in the morning (6-12 LT) sector, within a few degrees of the magnetic equator. These distributions of 50-500 eV electrons were anti-correlated with dense, cold plasma (e.g. the plasmasphere) as encountered by GEOS-2 in the afternoon sector *[Wrenn et al* 1979].

The uncertain relationship between the equatorially trapped ions and electrons was resolved by a survey of the AMPTE data, conducted by *Braccio* [1991]. (There are some limitations in the AMPTE data set used, primarily in the low energy limit of the spectral coverage (~10 eV for ions, 67 eV for electrons). This did not prevent a reasonably thorough look at the higher energy trapped distributions, but limits the information on other important distributions, particularly low energy field-aligned electrons.) This survey showed that the equatorially trapped ions and electrons overlapped in regions of occurrence, but that the peak occurrence probabilities were not in the same spatial regions. The peak occurrence probability for the trapped electrons was in the 6-12 LT sector, near geosynchronous orbit, as initially noted by the GEOS experimenters [*Wrenn et al,* 1979]. The ions, not mentioned in the GEOS reports, were primarily found at lower altitudes, hence the lack of mention of the phenomenon in reports of GEOS thermal ion measurements.

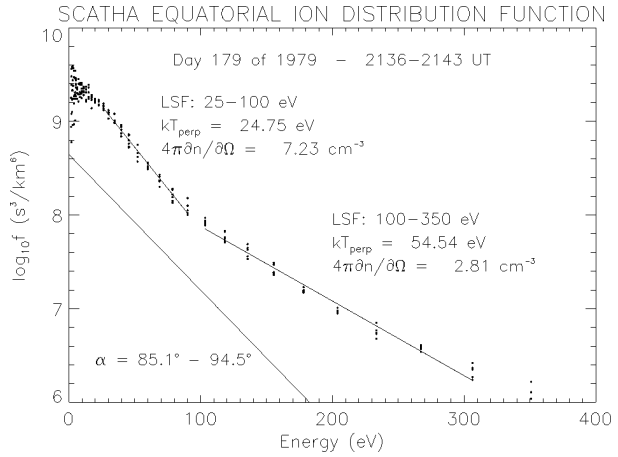

Figure 1. Ion distribution functions from the University of California at San Diego (UCSD) experiment on the SCATHA satellite are least square fitted over the indicated energy ranges.

The AMPTE survey showed the peak occurrence rate for the trapped ions was towards the afternoon sector, though this survey shared the problem found in the *Horwitz et al* [1981] ISEE survey - no coverage of the dusk bulge. Individual orbits showed ion and electron distributions confirming the statistical view on location - the locations for the peak flux for the trapped ion and electron distributions were offset. The peak in the trapped electron flux occurred radially outside the peak in the trapped ion flux, apparently outside the plasmasphere [*Braccio*, 1991].

One useful consequence of this survey, for our purposes, is that the trapped ion distributions found with DE 1 near $L = 4.5$ can be associated with isotropic electron distributions, in lieu of direct observations on that satellite. This scenario is particularly easy to model.

The basis of the model development presented here is that the core plasma distributions observed at the Earth's magnetic equator can often be described as bi-Maxwellian distributions. We begin by demonstrating that the near-geosynchronous SCATHA data, and the $L = 4.5$ DE 1 data can be described with such a distribution function. The use of data from two distinctly different detectors helps to remove any ambiguity as to how appropriate this description of the nature of the environment is.

SCATHA

Data from the electrostatic analyzers on SCATHA showed trapped distributions similar to those found earlier on ATS 6 and GEOS, but with substantially higher ion fluxes, and higher degrees of pitch angle anisotropy. *Olsen* [1981] noted that the ion and electron observations obtained near the magnetic equator, from L ~5.5 to 7, could be described as bi-Maxwellian, but did not demonstrate this. SCATHA data taken at 10 LT, $L = 5.5$, at the magnetic equator are used now to do so. The same data are used here as in that earlier work.

The electrostatic analyzers on SCATHA had a 5°×7° field of view, and 20% energy resolution. On this day (day 179 of 1979), the high-energy electron and ion sensors were viewing radially, while the low energy pair of electron and ion sensors viewed along the spin axis. The satellite spin axis was in the orbit plane, perpendicular to the earth-sun line. As a result, the radial detector sampled a full 360° pitch angle range. The sensors viewing along the spin axis sampled data at ~90° pitch angle.

The process used here is to fit both the energy and angular distributions. First, least square fits are done for the energy distributions at 90° pitch angle to obtain perpendicular temperature and density. Then the angular distributions are used to obtain the parallel temperatures. Figures 1 and 2 illustrate this process for the ions. Figure 1 shows the energy analysis at ~90° pitch angle (85°-94°, varying as the satellite spins). This analysis gives temperatures of 25 eV from 25-100 eV, and 55 eV from 100-350 eV. Note that the density obtained in such fits must be corrected for the effects of the satellite potential, and the anisotropy, hence the interim designation as $4\pi\,\partial\,n/\,\partial\,\Omega$. The diagonal line in the lower left corner is the isotropic background obtained from the subsequent analysis of the angular distributions.

Figure 2 shows the ion angular distributions taken at 41 and 103 eV. Pitch angle distributions such as these are available only for a limited set of energies where the radially viewing detectors are set to "dwell" for 60-s intervals (one satellite spin) [*Olsen*, 1981; Figure 7]. It is assumed that the ions are protons (a reasonable assumption, based on subsequent experience with DE 1 and AMPTE), and the distribution functions are plotted vs. the square of the cosine of the pitch angle. For a bi-Maxwellian, this will result in a straight line, just as plots of log F vs. energy do. Given the perpendicular temperature, the slope is then determined by the parallel temperature. The dotted lines show the fitted bi-Maxwellian

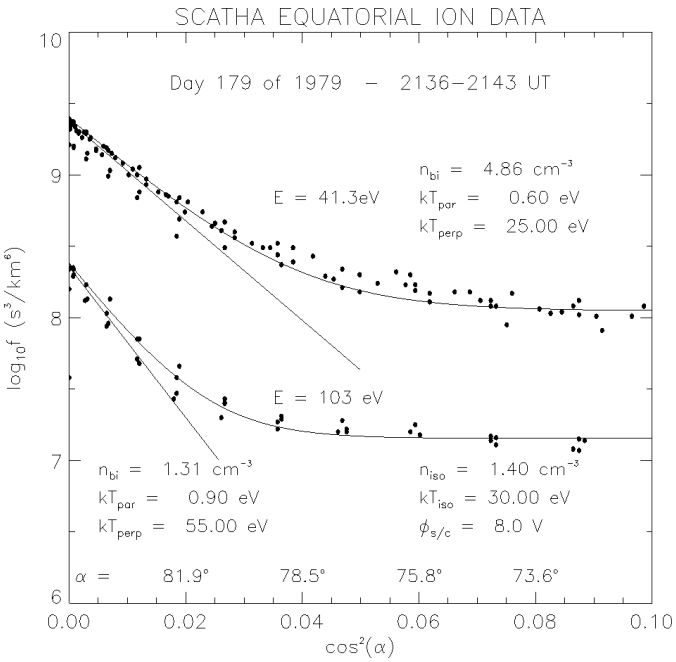

Figure 2. Ion pitch angle distributions from the UCSD experiment on the SCATHA satellite are fitted using a pair of bi-Maxwellian distribution functions, with the parameters indicated in the figure.

results. The presence of a warm isotropic background causes the curve to flatten at lower pitch angles (larger cos α). This term was added in, and results in the solid lines which overlay the two angular distributions. The parallel temperatures that result are 0.6 and 0.9 eV, for the two energy ranges noted above. This gives a temperature ratio of 42 for the central portion of the ion distribution.

The isotropic background ought to be included in the energy analysis of the 90° pitch angle data (Figure 1), but a plot of the inferred isotropic background distribution function (*f(E)*) in the lower left hand corner of Figure 1 shows that it is not a major term in the 90° pitch angle data (~10%).

Energy analysis of the 90° pitch angle electrons showed that the core of the distribution function could be described as a Maxwellian with T_{perp} ~20-25 eV, though even the data below 100 eV do not show a completely Maxwellian behavior. [*Scott,* 1991; Figure 17]. Figure 3 shows the angular analysis for the 41.3 eV electrons. The data centered at 90° pitch angle show the trapped distribution is not highly anisotropic at this energy, and the angular distribution is described by a parallel temperature which is ~75% of the perpendicular temperature. The anisotropy increases with energy; there is a higher temperature component (not shown here) which has kT_{perp} = 250 eV, kT_{para} = 19 eV, as found in the analysis of the 500 eV electrons [*Olsen*, 1981, Figure 8; *Scott,* 1991; Figure 19]. The core of the electron distribution function dominates the density, however, and this latter population is ignored, for now.

There is a field-aligned component in the electrons below ~20° pitch angle. The fit to the low-energy field-aligned electron data is somewhat more arbitrary, since there is effectively no energy analysis along the field line. Also, the ~0° and ~180° distributions differ slightly, and the fit is a compromise between the two ends of the pitch angle range. The anisotropy ratio is about 20, with a relatively small contribution to the total density. This portion of phase space appears to be associated with photo-electrons from the ionosphere.

There is a discrepancy between the total electron and ion densities, which is partly due to uncertainties in the instrument calibration at low energies, and partly due to degradation in the detector (channeltron decay). A portion of the difference is made up by the higher energy (E > 100 eV) electrons, and there may be a very low energy (E ~< 1 eV) plasma component that is not properly measured.

Dynamics Explorer 1

Dynamics Explorer 1 (DE 1) data established most clearly how the equatorially trapped ions were related to the plasmasphere, out to L = 4.5. The polar orbiting satellite provided latitudinal profiles of the trapped distributions, with instrumentation that allowed for mass analysis and total density measurements. The ion distributions were found to be primarily H^+, with 1-10% He^+, in density regimes of ~10-100 cm^{-3}, near the plasmapause [*Decreau et al*, 1986; *Olsen et al,* 1987]. Also, field-aligned density structures were identified in association with these trapped ion distributions, most notably a density minimum at the magnetic equator [Olsen, 1992].

Plate 1 shows the DE 1 data for 5 January 1984. The satellite is in a particularly suitable orbit, with apogee just above the equator. The satellite moves slowly in L, from ~4.8 to ~4.6,

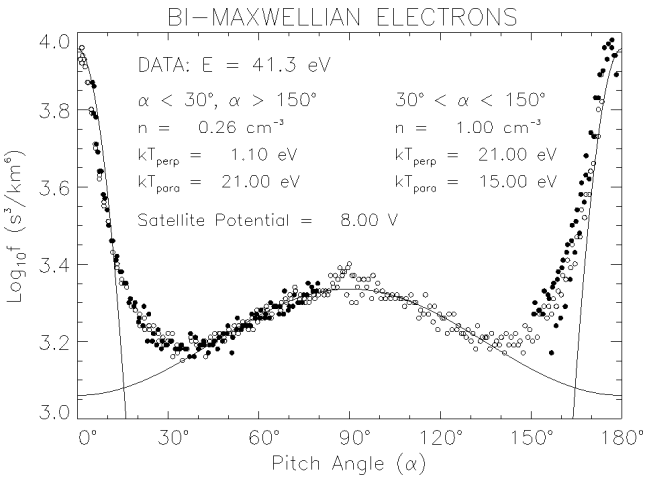

Figure 3. Electron pitch angle distributions from the UCSD experiment on the SCATHA satellite, from day 179 of 1979. Data are from the same time period shown in Figures 1 and 2. Data from the sunward sector are plotted as solid circles, data taken viewing in the antisunward direction are plotted as open circles. The data are overplotted with model bi-Maxwellian distributions.

as it passes from +15° to -15° magnetic latitude. The top two panels show the H^+ data, the 3rd and 4th panel show the He^+ data. The upper panel in each pair shows the spin-phase analysis of the data from the radially viewing sensor. The bottom panel in each pair show the 0 to 50-V RPA analysis from a sensor viewing along the spin axis (nominally at 90° pitch angle). In the spin-time panels, the horizontal white lines indicate the spin-phase associated with field-aligned measurements. The satellite is flying almost tangential to the magnetic field line. Hence, the data taken along the satellite velocity vector (ram, or 0° spin phase) corresponds to ~0° pitch angle.

The hydrogen and helium ion data show the characteristic trapped distribution seen ~50% (or more) of the time in the late afternoon [*Olsen et al*, 1987]. The hydrogen flux is 20-25 times higher than the helium flux; the helium density is about 10% of the hydrogen density. The bottom panel shows the total electron density obtained from the plasma wave instrument (PWI) measurements of the upper hybrid resonance [*Kurth et al,* 1979]. There is a peak in density at the equator, though part of the density rise is due to variations in "*L*".

Modeling the DE 1 ion data with bi-Maxwellian distributions can also be done, as with the SCATHA data. Such modeling requires careful consideration of the detector response, with integration in energy and angle, as opposed to the analysis of the almost differential electrostatic analyzer data shown above. Simple assumptions about constancy of the distribution function with angle cannot be made. The fitting process uses a model detector response, with the ability to specify an arbitrary ambient distribution function. *Biddle et al* [1985] used a similar approach to the RIMS data, for drifting Maxwellian distributions with a perturbing heat flux distribution. In this work, bi-Maxwellian distributions were specified.

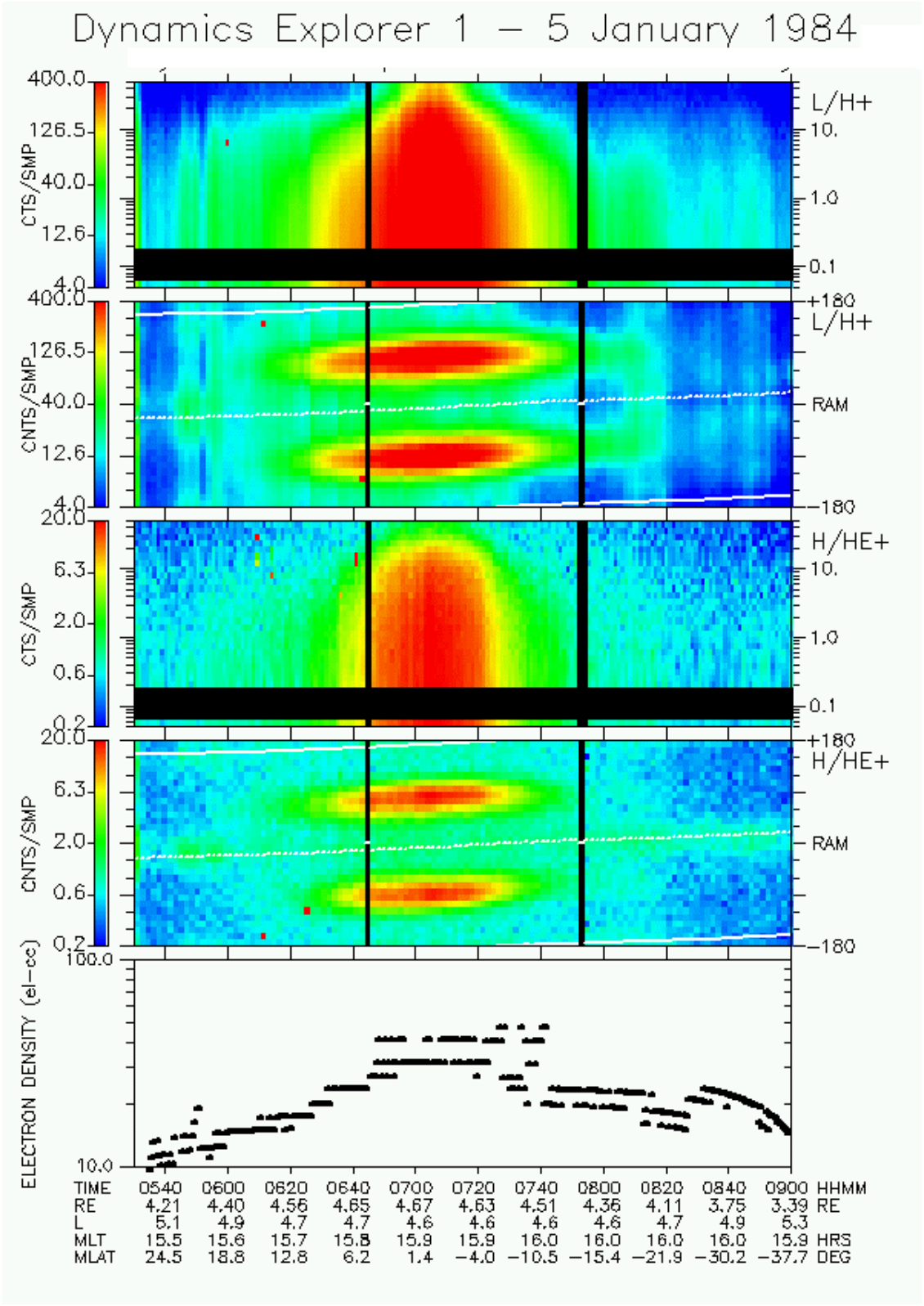

Plate 1. RPA time and spin phase time spectrograms for the DE 1 RIMS instrument. Data are shown from 0520-0900 UT, at ~1600 LT, as the satellite moves from +32° down to -37° magnetic latitude.

Data are used from the radial and end head (+Z) sensors. The radial detector has a ~20°x110° aperture, and provides data only at 0-V retarding potential. The sensor which views along the spin axis nominally measures 90° pitch angle particles, but the view angle is extremely wide – approximately 110°x110°. The RIMS model addresses the end head counts versus retarding potential analyzer (RPA) voltage and the radial head counts versus ram angle. The modeled RPA and spin curves are determined by solving the integral equation that relates the detector count rate to the view direction of the detector, the velocity space distribution function $f(\vec{v})$, the spacecraft potential and the RPA voltage.

The integration limits in velocity are functions of the incident direction of the particles, the energy dependent solid angle of the detector, the detector (+Z head or radial) and its settings, and the spacecraft potential and RPA voltage. The thin sheath approximation is used to compute the effect of the potential distribution around the satellite on the ambient plasma distribution [*Comfort et al,* 1982]. The velocity space distribution function was modeled by a bi-Maxwellian shifted into the spacecraft frame of reference.

The parallel and perpendicular temperatures and density were based on the best fit (minimum chi-squared) of the modeled curves to the RIMS data. This is an iterative process. First the +Z head data is fitted to obtain the perpendicular temperature. The shape of the +Z head model curves primarily depends on the perpendicular temperature, and is only mildly sensitive to the spacecraft potential or parallel temperature. The perpendicular temperature obtained from the +Z head was then fixed when fitting the radial head data to derive the parallel temperature. The parallel temperature is then obtained from a fit to the spin curve, and these parameters are used to correct the fit to the +Z data. The spacecraft potential can be returned as a fitted parameter in this process. For the results shown here, however, the known relation between potential and ambient plasma density was used as a constraint. This could be done because the total density was available from the plasma wave data [*Chappell,* 1988; figure 12].

Both the spacecraft potential and parallel temperature affect the shape of the spin curves (basically, the width). Because of this the minimum of chi-square for the radial head fit is not particularly sharp. Hence, there is a greater uncertainty in the parallel temperature estimate than the perpendicular temperature estimate. When the model was run without specifying the potential, the minimum chi-square was obtained for potentials near zero, and parallel temperatures from 1-2 eV, roughly half the values shown here. The density estimate is of limited accuracy because of uncertainty in the value of the spacecraft potential and detector sensitivity questions late in the mission. Since we have the total electron density, this aspect of the RIMS data was not pursued beyond the "uncalibrated" values given here.

Figure 4 shows the results of modeling the H^+ angular and energy distributions obtained at the magnetic equator. The top panel is a spin curve for the radially viewing detector, set at a retarding potential of 0 V. The spin phase (-180° to +180°) is roughly the pitch angle, at this time. The data are plotted as

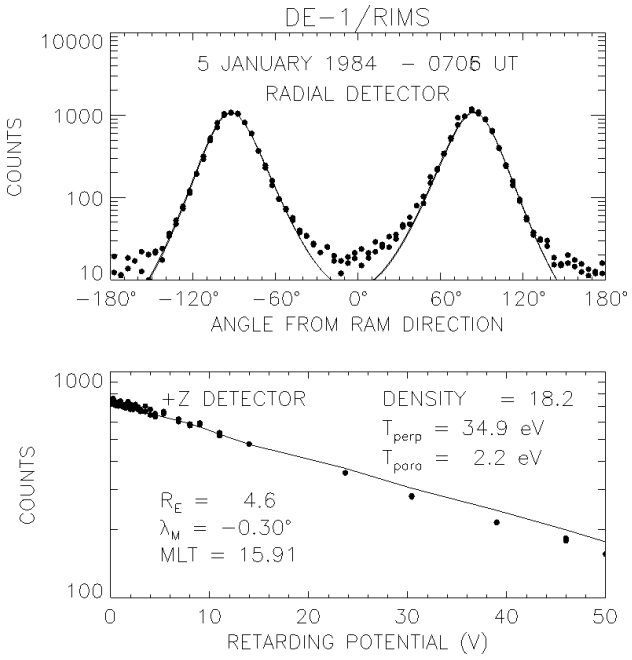

Figure 4. Ion spin-phase and RPA curves from the DE 1 retarding ion mass spectrometer (RIMS). The have been fitted with a bi-Maxwellian distribution function.

dots, the model as a solid line. This sensor accepts H^+ ions of energies of 0 eV up to ~250 eV (half-maximum). The bottom panel is the retarding potential analysis for data from a sensor viewing along the spin axis. The left hand portion ($-100°$ to 40°) of the spin curve was fitted. For the retarding potential analysis curve, the 0-25 V data were used in the fit. The fit parameters are: n = 18 cm^{-3}, T_{para} = 2 eV, T_{perp} = 33 eV, assuming a spacecraft potential of +3 V. Results for the latitude range of ±10° are presented below, with the modeling results.

These data from SCATHA and DE have shown that the equatorial plasma distributions can be described as bi-Maxwellians. This allows us to model the changes in the distribution function with latitude in a particularly nice way. One further aspect of the DE data must be addressed, first.

The existence of a peak in density at the equator needs some further consideration, before moving on to the model. This is done with a plot of the data vs. L, as shown in Figure 5a. Figure 5b shows the satellite orbit for the same period. The data taken south of the equator are plotted as a solid line in the top figure. The satellite reaches minimum L at L = 4.57, λ = -8.4 . Data taken past this point are plotted as open circles. There is a general trend of L^{-4}, as is often found. As the minimum L point is approached, the density runs sharply upward. This occurs as the satellite crosses the equator. The deviations from the L^{-4} curve are due to latitude effects, not radial structure. The existence of a peak in density at the equator is rare in the DE data set, but not unique. *Scott* [1991] shows a second example.

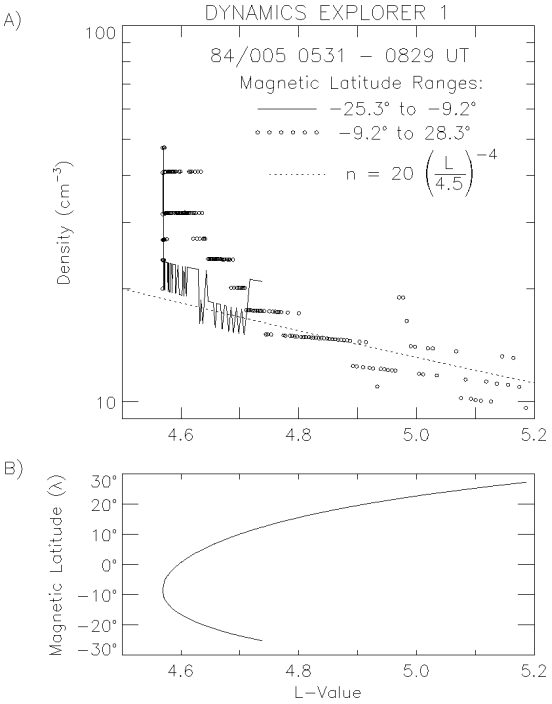

Figure 5. DE 1 total electron density profile versus L.

SELF-CONSISTENT FIELD AND PARTICLE DISTRIBUTIONS

Our objective is to use the measurements of the equatorial particle distributions to obtain the parallel electric field structure and the evolution of the plasma distribution function along the field line. Appropriate use of kinetic theory allows us to use the measured (and inferred) particle distributions to obtain the electric field, and hence the variation in plasma density along the magnetic field line. The approach, here, is to utilize the adiabatic invariants, and assume the plasma distributions are in equilibrium. This seems to be a reasonably good assumption - the trapped plasma distributions generally appear reasonably stable over the several hour period required by DE to travel through such regions. Another way of expressing this constraint on the model is that the change in particle energy during one bounce should be small compared to the particle energy ($\Delta E/E << 1$). There is also a constraint on pitch angle scattering; the bounce averaged change in pitch angle needs to be "small" ($\Delta\alpha \tilde{<} 1°$)

Of course, the distributions can't be totally stable - the $T_\perp/T_{||} >> 1$ condition identified above is presumably due to fairly intense wave-particle-interactions (wpi). The question is then one of time scales. *Lin et al* (1992) show how for nominal levels of wave activity, the latter stages of refilling (nominally our condition), the rate of change for characteristic parameters such as temperature are relatively slow - minutes to tens of minutes. By contrast, the equilibration time for the electric field would be determined, as a worst case, by processes occurring at the Alfven speed or ion sound speed - both in the 10-100 km/s range. The phenomenon under study has characteristic distances of 1-2 R_E (~10,000 km). This gives a time scale of 100-1000 seconds for the system to reach an equilibrium. This is only slightly less than the time scale identified by Lin et al [1992], for changes to occur in the thermal plasma. If the quasi-static theory is to be applicable, the potentials need to be mediated by faster processes, mediated by the electrons. Such processes are 10-1000 times more rapid, and the ultimate successes here in matching the data to theory suggest that such processes must be occurring.

The idea of looking at the consequences of non-isotropic particle distributions for parallel electric fields is not a new one. *Swann* [1933] set the basis for this work by showing how, in a collisionless plasma, the distribution function remains invariant for motion along a magnetic field line. This concept found early application in studies of the radiation belts [*Lundquist et al,* 1962].

Alfven and Falthammar [1963], and *Persson* [1963; 1966] showed how differences in the ion and electron pitch angle distributions require the existence of a parallel electric field, in a collisionless plasma. The classic article on this topic is the examination of ionosphere-magnetosphere coupling by *Chiu and Schulz* [1978]. This work includes ionospheric electrons, bi-Maxwellian distributions for the hot magnetospheric plasma, and the backscattered hot plasma, and develops the forms for the resulting density and potential profile. The development by Chiu and Schulz pays particularly close attention to the question of excluded regions in phase space, and the constraints this imposes on the shape of the modeled electric field. One minor difference with the emphasis pursued here, is that the anisotropy studied by these authors was postulated to occur in the hot electrons, with $T_\perp/T_{||} > 1$. In the work developed here, the anisotropy of interest is in the ions.

More recently, *Huang and Birmingham* [1992] looked at the behavior of (essentially) plasmaspheric distributions in rotating systems, including the effects of gravity. Huang and Birmingham develop electric field, density, and temperature relationships very similar to those developed below, and previously obtained by *Scott* [1991].

Whipple [1977] set up a useful formalism for studying the problem, based on the use of the invariance of the total energy, and the first adiabatic invariant, μ. If quasi-neutrality is invoked, it is possible to obtain an expression for the electric field. These integrals are relatively straightforward for bi-Maxwellian distributions. A surprising amount can be done even without integration. The results of such calculations are presented below, studied using parameters from SCATHA and DE 1, and compared with data from DE 1.

A Kinetic Model

It might be expected that the shape of the distribution function would change as the plasma distribution moves away from the equator. It can be shown, however, that the shape of the distribution function remains that of a bi-Maxwellian, even with a parallel electric field. The parallel temperature remains constant, while the perpendicular temperature drops.

The particle distribution function for both species is taken to be a bi-Maxwellian at the magnetic equator. The subscript "o" is used to designate the equatorial functions and parameters.

$$f_o\left(\vec{v}_o\right) = n_o \left(\frac{m}{2\pi\, kT_{\perp o}}\right)\left(\frac{m}{2\pi\, kT_{\parallel}}\right)^{\frac{1}{2}} \quad (1)$$
$$\bullet \exp-\left(\tfrac{1}{2}mv^2_{\perp o}/kT_{\perp o} + \tfrac{1}{2}mv^2_{\parallel o}/kT_{\parallel}\right)$$

The particle distribution function can be mapped off the equator by solving for particle velocities at the equator in terms of the "off-equator" values. Liouville's theorem can then be invoked to obtain the distribution function at any latitude (subscript λ).

The particle's velocity at the equator $\left(\vec{V}_o\right)$ can be expressed in terms of the velocity at any point along the field line $\left(\vec{V}_\lambda\right)$ using conservation of energy (E) and the magnetic moment μ:

$$\tfrac{1}{2}\, mv^2_{\perp o} = \mu\, B_o \quad (2)$$
$$\tfrac{1}{2}\, mv^2_{\perp o} = \tfrac{1}{2}\, mv^2_{\perp \lambda}\ \left(B_o\ /B_\lambda\ \right)$$
$$\tfrac{1}{2}\, mv^2_{\parallel o} = E - \mu\, B_o + q\phi \quad (3)$$
$$\tfrac{1}{2}\, mv^2_{\parallel o} = \tfrac{1}{2}\, mv^2_{\perp \lambda}\ \left(1 - B_o\ /B_\lambda\right) + \tfrac{1}{2}\, mv^2_{\parallel \lambda}\ + q\phi$$

The use of Liouville's theorem:

$$f_\lambda\ \left(\vec{v}_\lambda\right) = f_o\ \left(\vec{v}_o\left(\vec{v}_\lambda\right)\right) \quad (4)$$

allows the distribution function at a magnetic latitude λ_m , to be obtained by substituting the expressions found in equations 2 and 3 into equation 1. Combining terms, we can obtain

$$f_\lambda\ \left(\vec{v}_\lambda\right) = n_\lambda\ \left(\frac{m}{2\pi kT_{\perp\lambda}}\right)\left(\frac{m}{2\pi kT_{\parallel}}\right)^{1/2} \times \quad (5)$$
$$\exp-\left(\tfrac{1}{2}mv^2_{\perp\lambda}\ /kT_{\perp\lambda}\ + \tfrac{1}{2}mv^2_{\parallel\lambda}\ /kT_{\parallel}\ + q\phi/kT_{\parallel}\right)$$

The new distribution function still has the form of a bi-Maxwellian distribution, aside from restrictions due to accessibility, addressed below. The parallel temperature is unchanged, while the perpendicular temperature varies according to the form::

$$kT_{\perp\lambda}\ = \frac{kT_{\perp o}}{kT_{\perp o}/kT_{\parallel}\ + B_o/B_\lambda\ \left(1 - kT_{\perp o}\ /kT_{\parallel}\ \right)} \quad (6)$$

The new perpendicular temperature is a simple function of the equatorial temperatures, and the change in magnetic field strength. Note that the perpendicular temperature ($T_\perp$) will approach the parallel temperature ($T_\parallel$) as latitude increases. Note that if there are excluded regions in the distribution function, as discussed below, the temperature defined here will not be the average energy, as defined by the energy moment. It is, however, the quantity which would be defined by energy analysis of observed distributions, and precisely the term which needs to be compared to data.

The result that the bi-Maxwellian form is maintained is a result of the fact that the distribution function depends on pitch angle only through the sine function. The invariance of μ means that $\sin^2(\alpha)$ varies linearly with magnetic field strength. This is more obvious in the case of energetic particle distributions, which are traditionally treated as depending on the product of a power law and powers of sin α, [e.g., *Cladis et al,* 1961; *Freeman,* 1962; *Fritz and Williams,* 1973; *Blake et al* 1973; *Guzik et al,* 1989]. Distribution functions which vary as $\sin^m\left(\alpha\right)$ f(E) will not change in their angular distribution; the density simply decreases with latitude as long as m > 0.

The density is, as always, the integral of the distribution function over the allowed region of phase space. The main concern is to properly evaluate the lower limits of integration. *Whipple* [Figure 1, 1977] shows the two possibilities - particles in a potential well (electrons, in our case), and particles above a potential barrier (ions, in our case). *Chiu and Schulz* [1978] provide a similar analysis. Plate 2 illustrates for ions. The lower portion of Plate 2 shows a bi-Maxwellian distribution function, with reasonably typical parameters ($T_\perp$ is a little low, to avoid an excessively elliptical plot). The top portion of Plate 2 shows the same distribution, mapped through a 1.04-V potential drop to 20° magnetic latitude. The black region in the center represents ions with velocity coordinates which cannot reach the equator. This region of "equatorially excluded" velocities is due to the restriction that the total energy, E (which is kinetic plus potential energy), be greater than μB_o [*Whipple*, Figure 1b, 1977]. The region is delimited by the ellipse defined by the equation:

$$-q\phi\ = \tfrac{1}{2}mv^2_{\parallel\lambda}\ + \tfrac{1}{2}mv^2_{\perp\lambda}\ \left(1 - B_o/B_\lambda\right) \quad (7)$$

The eccentricity of the ellipse is greatest near the equator, and drops toward one at high latitudes. The white circle shows the less restrictive conservation of energy condition, $E = -q\,\phi$.

Other elements of the mapping process are indicated in the lower panel by the diagonal lines, which show the limits for mirroring in the absence of an electric field (the traditional mirror equation) (α = 50°, here). The hyperbolic traces show the limits for mirroring with the electric field, and the mirror region is labeled with the capital M. The hyperbola maps to the horizontal white line in the top panel. Conversely, the ellipse in the top panel maps to the V_{para} axis of the bottom panel.

With the limits of integration determined, the distribution function can be integrated to obtain:

$$n_\lambda = n_o\ \left(kT_{\perp\lambda}/kT_{\perp o}\right)\exp\left(-q\phi/kT_{\parallel}\right)(1 - C) \quad (8)$$

The familiar Boltzmann factor appears, along with the temperature ratio, determined in equation 6. There is an additional correction term, C, which is 0 for the case of q > 0 (electrons, in our problem), and which is given by equation 9 for the case of q < 0 (ions, in our problem). This term is basically the integral over the equatorially excluded (forbidden) region.

$$C = \operatorname{erf}\sqrt{-q\phi/kT_{\parallel}}\ - \frac{2}{\sqrt{\pi}}\frac{\exp\left(q\phi/kT_{\parallel}\right)}{\sqrt{\dfrac{1}{B_\lambda/B_o - 1}\ \dfrac{kT_{\parallel}}{kT_{\perp o}}}}\ D\left(\sqrt{\frac{1}{B_\lambda/B_o - 1}\ \frac{-q\phi}{kT_{\perp o}}}\right) \quad (9)$$

Here, D(x) is Dawson's integral: $D(x) = e^{-x^2} \int_0^x e^{t^2}\, dt$ [*Abramowitz and Stegun,* 1965, p 319], which is closely related to the error function of an imaginary argument. This term has the effect of further reducing the density, for a distribution with a density that is already dropping due to mirror effects. It also makes the remainder of the solution for an analytic, self-consistent potential/density profile impossible. In order to maintain that aspect of the work, and to match our subsequent approach of analyzing the RIMS data as a bi-Maxwellian at all latitudes, we have chosen to take the "forbidden" region as having been filled during the slow (compared to a bounce period) development of the potential structure in the mirror geometry. Also, if there were a hole in the distribution function, some form of instability would doubtless act to diffuse particles into that region of phase space. These particles are trapped away from the equator, and are not observable at the equator We take the distribution function in the forbidden region to have the values defined by equation 5. This portion of the distribution function will, in general, be difficult to observe due to satellite charging effects, and this assumption will not affect the parameters obtained in the DE 1 analysis. We are effectively taking the correction factor, C, as zero for both species.

For simplicity, we restrict the presentation here to the case of a bi-Maxwellian electron distribution, and a single bi-Maxwellian ion distribution. Inclusion of multiple species or an isotropic background has been done, but the equations are not terribly illuminating. *Scott* [1991] shows that in general, the effect of an isotropic background is simply to reduce the slope of the density profile, and hence the magnitude of the electric field. We continue by assuming charge neutrality, and solve for the potential:

$$e\phi = \frac{kT_{\parallel i}\, kT_{\parallel e}}{kT_{\parallel i} + kT_{\parallel e}} \ln\left(\frac{1 + \left(B_\lambda/B_o - 1\right)\, kT_{\perp e\, o}/kT_{\parallel e}}{1 + \left(B_\lambda/B_o - 1\right)\, kT_{\perp io}/kT_{\parallel i}}\right) \qquad (10)$$

This form shows immediately that if both species have the same anisotropy ratio, there is no electric field (as in *Alfven and Falthammar* [1963]), and that if the ion (electron) anisotropy ratio is greater than one, the potential at the equator is a maximum (minimum). The magnitude of the potential tends to scale with the lower of the two parallel temperatures, and the sign depends on the two temperature (anisotropy) ratios.

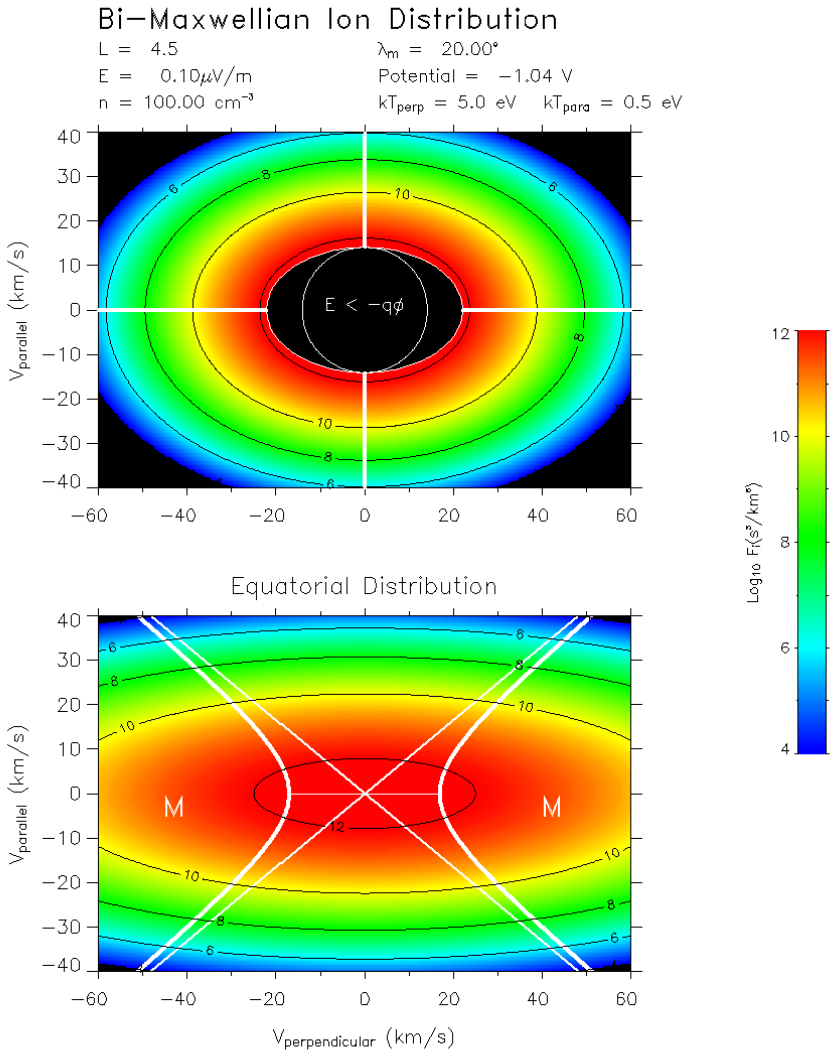

Plate 2. Distribution function plots for a bi-Maxwellian distribution.

Consequences Of The Model

We now briefly explore the consequences of these simple results for the sorts of plasma parameters obtained in the previous sections. Figure 6 illustrates how the perpendicular temperature varies with latitude for the ion plasma parameters found above in the SCATHA data. The initial perpendicular temperature, 25 eV, has dropped to less than 5 eV at 10° magnetic latitude, and is rapidly approaching an asymptotic value that is the parallel temperature. This explains the substantial difference in the character of the distributions measured by ATS-6, at 10° magnetic latitude, and SCATHA, at the equator. The temperature profile obtained from DE 1 will be compared to this model below.

The density will vary in precisely the same way, in the absence of an electric field. Temperature anisotropy ratios $\left(T_{\perp}/T_{\parallel}\right)$ greater than one result in a density peak at the equator, ratios less than unity, result in a minimum in density. Figure 7a shows how the density would vary, in the absence of an electric field, for a range of anisotropies. These are the density profiles which would be observed in either specie, if the electron and ion anisotropies were the same.

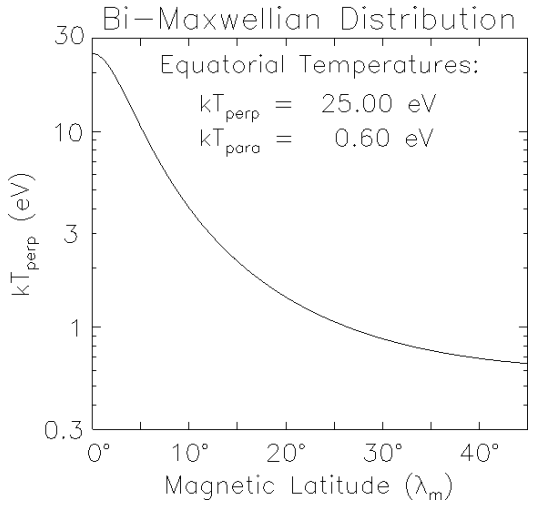

Figure 6. Variation in temperature with latitude, for ion plasma paraqmeters noted in Figure 2.

Adding the electric field to the problem requires specification of the parallel and perpendicular temperatures for both species. For simplicity, we set the electron distribution to be isotropic. By way of justification, and in the absence of DE 1 electron data at $L = 4.5$, we cite the survey by *Braccio* [1991], who showed that the equatorially trapped electron distributions were primarily found outside the plasmasphere, in the 0600-1200 LT sector. To further simplify the presentation, we choose the electron temperature equal to the parallel ion temperature.

The density and potential profiles of Figures 7b and 7c result if the electron temperature is set to 1 eV. The self-consistent density profiles, shown in Figure 7b, still vary with latitude, but not as rapidly as found in the absence of an electric field (Figure 7a). The electric field which results from quasi-neutrality requirements can never produce an effect which is greater than the effect of the anisotropy hence the electric field is never strong enough to counteract the decrease in density with latitude implied by a pancake distribution, for an isotropic electron background.

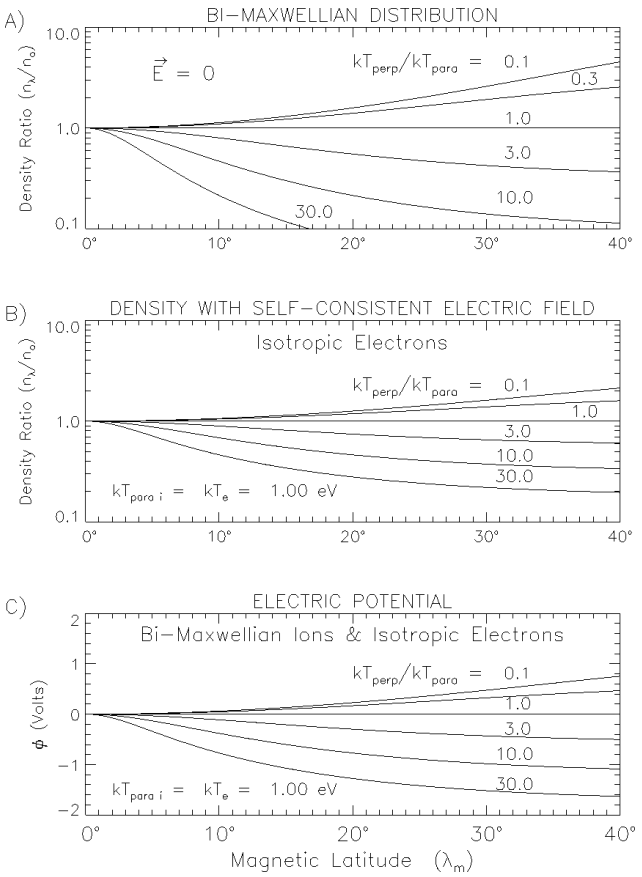

Figure 7. (a) Density profiles for bi-Maxwellian distributions in a dipole mirror geometry. (b) Density profiles for bi-Maxwellian ion distributions with an isotropic background. (c) Electric potential profiles associated with Figure 7b.

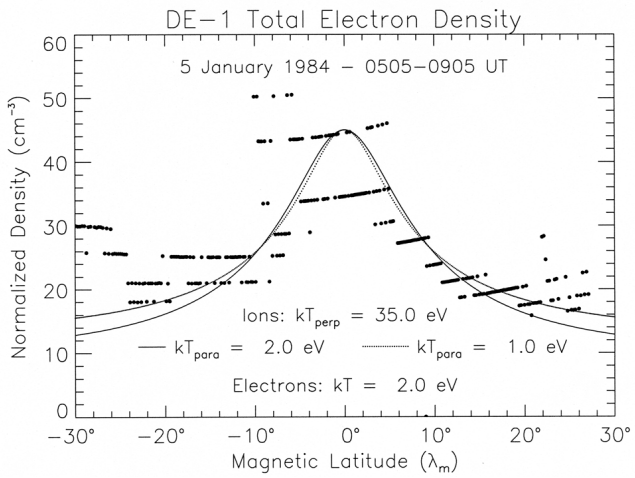

Figure 8. DE 1 total electron density, normalized to L = 4.5, compared to the kinetic model.

The electric potential associated with these density profiles is shown in Figure 7c. Potential drops of 1-2 V are found. The remarkable similarity between figures 7b and 7c is due to the fact that the (electron) density and potential are related by the Boltzmann relation. Note that the potentials are roughly proportional to the parallel electron temperature; higher temperatures will give larger potential drops. Referring to Equation 10, we note that in general the potential will scale with the lower of the parallel temperatures. [See also, *Scott,* 1991, figure 28] The electric field can be obtained by differentiating, and values of about 0.1 μV/m are obtained, peaking at 5-10° magnetic latitude. Such potentials have been proposed as an explanation for the changes in field-aligned ion behavior in the DE 1 data set. *Olsen et al* [1987] show data in which there is either a gradual fade in the intensity of field-aligned flows [*Olsen et al,* 1987; Plate 3], or what appears to be field-aligned ion beams bouncing off a potential structure [*Olsen et al*, 1987; Plate 5].

Numerical evaluation of the potential vs. latitude with the distribution function set to zero in the forbidden region gave potentials a factor of 2 or so higher in magnitude away from the equator, but no major qualitative difference.

Comparison With Data

Trapped Ions and Isotropic Electrons: Density Minimum

We now compare the DE 1 data from 5 January 1984 to the model. Figure 8 shows the total electron density, normalized by $(L/4.5)^4$, so that in principle only the latitudinal effects will be present. This normalization is supported by the slope found in the off-equator data (Figure 5), and has been used previously [*Olsen*, 1992]. For the model, the ion plasma parameters are taken from the fit to the equatorial data (Figure 4).

The electron temperature is set equal to the parallel ion temperature (2 eV), and the density profile, with self-consistent electric field, is obtained (the solid line). The SCATHA data, and additional work with the RIMS model, suggest that the parallel ion temperature is too high, so we also show the results for a parallel ion temperature of 1 eV (holding the electron temperature at 2 eV). The results are not greatly different; the dotted line is narrower (drops a little more quickly) near the equator, and runs slightly above the solid line for latitudes above 10°. Note that with the above choices made on the basis of the plasma data, there are no free parameters to adjust. The agreement appears to be good. By comparison with figure 7, in the absence of an electric field the density profile would be substantially narrower than the observed density distribution. If the electric field had not been included, a much lower model anisotropy would have been needed to match the data.

Figure 9 shows how the ion plasma parameters vary with latitude, and compares them to the model. The data analysis showed a drop from ~30 eV perpendicular temperature to ~10 eV. This occurs in less than 10° travel away from the equator. The parallel temperature remained constant at ~2 eV. There were some indications in the analysis that this temperature was too high. Note that it is about double the value found with the SCATHA data. The density obtained in the fit of the bi-Maxwellian ions is given in the bottom panel. Aside from some instrument sensitivity questions during this period, this value should be reasonably close to the total ion density at the equator. This is because the trapped distribution is the bulk of the plasma, and the temperature is high enough to overcome any charging effects. Away from the equator, the temperature drops, and the isotropic ("hidden") background becomes more important [*Olsen et al*, 1985].

The fitted temperatures and density are overlaid with the curves determined solely by the equatorial measurements. The $T_\perp/T_\parallel$ ratio of 18 is the value generated by the equatorial measurements. A ratio of 40 appears to more closely match the variation in ion temperature observed in the ion data. Note that this aspect of the model does not depend on the electron

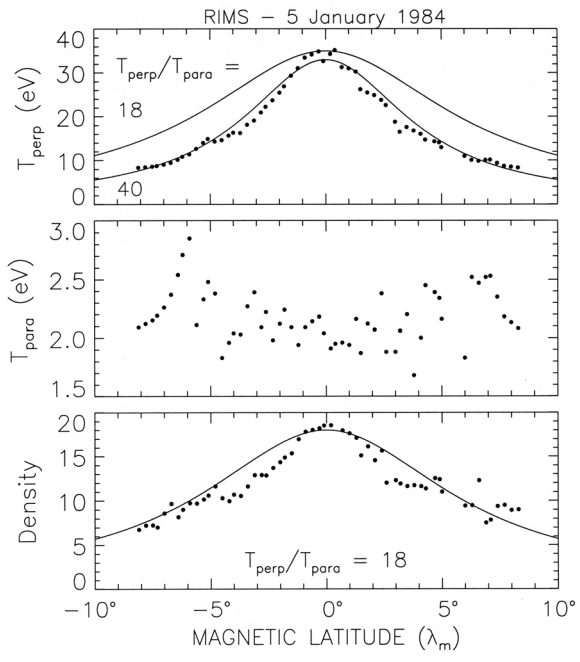

Figure 9. DE 1 ion temperature data from 84/005, compared with kinetic model.

characteristics (and by implication, the electric field), or on the effects of an isotropic background - only on the temperature ratio at the equator. This comparison of model and data suggests that the parallel ion temperature is closer to ~0.8 eV than 2 eV. The former value is close to that found for the SCATHA data shown here, and a much more typical value for the isotropic plasma of the outer plasmasphere [*Olsen et al*, 1985].

The density decrease expected in the absence of an electric field (equation 8, figure 7a) is overlaid on the ion density estimate. It describes the variation in density of the trapped plasma reasonably well - the effects of the electric field are fairly modest close to the equator. The simple kinetic model for the variation in a bi-Maxwellian ion distribution gives a remarkably good agreement with the latitudinal profiles of temperature and density, for this case where there is a maximum in density at the magnetic equator.

These results are similar to those obtained by Singh and Torr [1990] in a model of plasmasphere filling. Singh and Torr solve a time-dependent hydrodynamic model with equatorial ion heating, and find a quasi-steady state density profile which is similar to that shown here - peaked within 10° of the equator. Singh and Chan [1992] extend the application of the hydrodynamic code, again with similar results. In the same work, Singh and Chan show how in a kinetic simulation a potential maximum builds up near the equator early in the refilling process, as does the density. A density minimum occurs only later in the simulation.

The kinetic simulation by Lin et al [1992] provides a latitudinal temperature profile similar to those found here, in a time-dependent model. This model introduces wave heating in a narrow latitudinal range near the equator, producing plasma distributions very similar to those reported here for the magnetic equator. The Lin et al density distributions are somewhat less clear in their relationship to the data shown here - there is more structure in the simulation profile, including a dip just at the equator.

Traped Ions and Field Aligned Density Minimum

The remaining problem is how to explain the occurrence of a density minimum at the magnetic equator, or even a flat density profile, in the presence of trapped ion distributions. The answer is that flat density profiles are possible in the presence of field-aligned electron distributions - that is electron distributions which are either beam-like, or bi-Maxwellian distributions with $T_{\parallel}$ greater than $T_{\perp}$. As shown above, in Figure 7a, the presence of field-aligned distributions will result in a density minimum at the equator. If the electron distribution is field-aligned, and the ion distribution is trapped, the effects can cancel, via the electric field.

The SCATHA data described above show such characteristics, as do recently received data from the geosynchronous satellite, 1989-046. *Laszakovits* [1993] analysed low-energy (E < 100 eV) electron data from the 1989-046 satellite, and found that field-aligned distributions were a ubiquitous feature at geosynchronous orbit, even on the night side. Based on this experience, it seems appropriate to further model the DE 1 density profiles, using trapped ions and field-aligned electrons.

Data were chosen from a previously published example, from 18 July 1982 [*Olsen*, 1992]. DE 1 is in an orbit which varies in *L* from 4.7 to 5.1 during the majority of the period of interest. Electron densities obtained from the plasma wave data are plotted in Figure 10, normalized by L^4. Electron plasma parameters for the model were based on the values in figure 3; ion values were somewhat arbitrarily set at generic values, since the ion temperature analysis was unavailable. The density minimum in the model follows a curve that is suprisingly close to the data. (The divergence between theory and model for $|\lambda| > 30°$ occurs as *L* increases past 5.5). Results for a second example (83/296, also from *Olsen* [1992]) were similar. In both cases, the only parameter which was adjusted for a fit was the equatorial density.

Summary and Conclusions

The plasma distributions found in the outer plasmasphere can often be described as bi-Maxwellian distributions, at least for the core of the distribution. Specification of the full distribution function at the equator allowed us to develop a kinetic model for the variation in the ion temperature and density with latitude. Comparison of the model with DE data shows that for an isotropic electron background, there will be a local maximum in density at the equator, which is reasonably well described by the model. A density profile with a minimum at the equator requires opposing anisotropies in the ions and electrons.

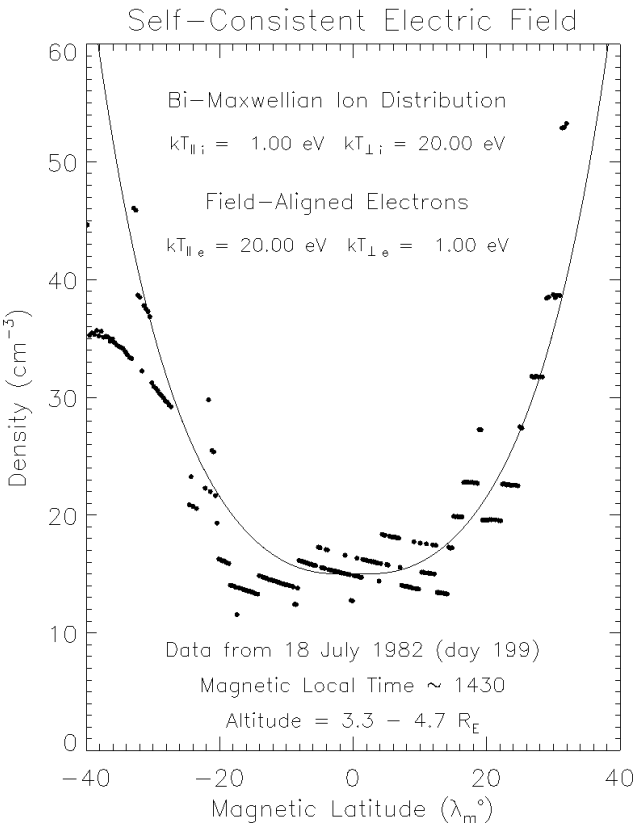

Figure 10. Electron density profiles, for bi-Maxwellian distributions with pancakelike ions, and field-aligned electrons. Data from Dynamics Explorer 1, on day 199 of 1982.

In all cases the inferred potential drops in the equatorial region is only 1-2 V, since the parallel ion temperature is relatively low. Still, such potentials may be adequate to explain the apparent repulsion of low-energy field-aligned ion beams from the equatorial region.There are a number of problems with the present development, in spite of our apparent success in explaining the data. First of all, the energy distribution is not that well defined by a single slope (e.g. one temperature). A suprathermal tail is present, and not well accounted for. It was a problem in the analysis, and makes it difficult to fit a bi-Maxwellian to plasma data over broad energy ranges. Some sort of Kappa function (e.g. a generalized Lorentzian) fit might very well be warranted, and there are ongoing studies about implementing such fits for the DE/RIMS data [*Vasyliunas,* 1968; *Christon et al* 1988, 1991]. These calculations should eventually be redone for those more realistic distributions, as with recent work in plasma waves [*Summers and Thorne*, 1992].

In addition, the hot plasma background ought to be included, as with studies associated with auroral features. [*Galperin and Volosevich*, 1989]. Calculations involving more than two distributions become non-analytic, however, and fairly promptly become the proper domain of numerical simulation. It can be stated that the lowest (parallel) temperature distribution tends to dominate, however. The effect of the field-aligned potential is most dramatic for the core distribution, and the density gradients which balance the electric field are most directly involved for these particles. Also, the anisotropy of the hot plasma tends to be relatively low, and the dayside (6-18LT) hot plasmas (the region for which data have been used) are relatively diffuse.

Finally, though of great value in demonstrating the important physical mechanisms at work in the outer plasmasphere, this work suffers from the quasi-static nature of the solution. There is a stage well beyond this work that will involve the application of models such as that of *Lin et al* [1992] to direct comparison with time varying measurements of all the pertinent plasma quantities. At that point, the many assumptions and guesses made here can be set aside.

ACKNOWLEDGEMENTS

The principal investigator for RIMS was C. R. Chappell. He and Tom Moore provided access to the RIMS data. Tom Moore gave us substantial help in implementing the RIMS detector response model. Don Gurnett (Univ. of Iowa), was the principal investigator for the plasma wave instrument. Our thanks go to J. L. Horwitz for keeping our kinetic theory straight. Thanks go to Joe Fennell, Walker Fillius, Charles Lundquist, and Don Williams for help in tracking down the origins of the field-aligned mapping process. This work was completed while one of us (RCO) was a NASA/ASEE Summer Faculty Fellow at NASA/MSFC. This work was done while S. A. Boardsen held a National Research Council - Marshall Space Flight Center Resident Research Associateship.

The editor thanks J. L. Horwitz and an other referee for their assistance in evaluating this paper.

REFERENCES

Abramowitz, M., and I. A. Stegun, Handbook of Mathematical Functions, Dover Publications, NY, NY, 1965.

Alfven, H., and C.-G. Falthammer, Cosmical Electrodynamics, Fundamental Principals, p 164, Clarendon, Oxford, 1963.

Biddle, A. P., T. E. Moore, and C. R. Chappell, Evidence for ion heat flux in the light ion polar wind, *J. Geophys. Res., 90 ,* 8552-8558, 1985.

Blake, J. B., J. F. Fennell, M. Schulz, and G. A. Paulikas, Geomagnetically trapped alpha particles, 2. The inner zone, *J. Geophys. Res.*, *78 ,* 5498-5506, 1973.

Braccio, P. G., Survey of trapped plasmas at the Earth's magnetic equator, MS. Thesis, Naval Postgraduate School, Monterey, CA, December, 1991.

Chappell, C. R., The terrestrial plasma source: A new perspective in solar-terrestrial processes from Dynamics Explorer, *Rev. Geophysics., 26* , 229-248, 1988.

Chiu, Y., T., and M. Schulz, Self-consistent particle and parallel electrostatic field distributions in the magnetospheric-ionospheric auroral regions, *J. Geophys. Res., 83,* 629-642, 1978

Cladis, J. B., L. F. Chase, W. L. Imhof, and D. J. Knecht, Energy spectrum and angular distributions of electrons trapped in the geomagnetic field, *J. Geophys. Res.*, *66,* 2297-2312, 1961.

Comfort, R. H. and J. L. Horwitz, Low-energy ion pitch angle distributions on the dayside at geosynchronous altitudes, *J. Geophys. Res., 86* , 1621-1627, 1981.

Comfort, R. H., C. R. Baugher, and C. R. Chappell, Use of the thin-sheath approximation for obtaining ion temperatures from the ISEE 1 limited aperture RPA, *J. Geophys. Res., 87,* 5109-5123, 1982.

Christon, S. P., D. G. Mitchell, D. J. Williams, L. A. Frank, C. Y Huang, and T. E. Eastman, Energy Spectra of plasma sheet ions and electrons from ~50 eV/e to ~ 1MeV during plasma temperature transitions, *J. Geophys. Res., 93*, 2562-2572, 1988

Christon, S. P., D. J. Williams, D. G. Mitchell, C. Y Huang and L. A. Frank, Spectral characteristics of plasma sheet ion and electron populations during disturbed geomagnetic condtions, *J. Geophys. Res., 96*, 1-22, 1991

Decreau, P. M. E., D. Carpenter, C. R. Chappell, R. H. Comfort, J. Green, R. C. Olsen, and J. H. Waite, Latitudinal plasma distribution in the dusk plasmaspheric bulge: Refilling phase and quasi-equilibrium state, *J. Geophys. Res., 91,* 6929-6943, 1986.

Freeman, J. W., Detection of an intense flux of low-energy protons or ions trapped in the inner radiation zone, *J. Geophys. Res*., *67,* 921-928, 1962.

Fritz, T. A., and D. J. Williams, Initial observations of geomagnetically trapped alpha particles at the equator, *J. Geophys. Res*., *78,* 4719-4723, 1973.

Galperin, Yu. I, and A. V. Volosevich, The ARCAD-3 project and the theory of auroral structures, *Can. J. Phys., 67*, 719-732, 1989.

Guzik, T. G., M. A. Miah, J. W. Mitchell, and J. P. Wefel, Low-altitude trapped protons at the geomagnetic equator, *J. Geophys. Res., 94,* 145-150, 1989.

Horwitz, J. L., and C. R. Chappell, Observations of warm plasma in the dayside plasma trough at synchronous orbit, *J. Geophys. Res., 84*, 7075-7090, 1979.

Horwitz, J. L., C. R. Baugher, C. R. Chappell, E. G. Shelley, and D. T. Young, Pancake pitch angle distributions in warm ions observed with ISEE 1, *J. Geophys. Res*., *86,* 3311-3320, 1981.

Huang, T. S., and T. J. Birmingham, The polarization electric field and its effects in an anisotrpic rotating magnetospheric plasma, *J. Geophys. Res., 97,* 1511-1519, 1992.

Kurth, W. S., J. D. Craven, L. A. Frank, and D. A. Gurnett, Intense electrostatic waves near the upper hybrid resonance frequency, *J. Geophys. Res., 84,* 4145-4164, 1979.

Laszakovits, J. S., Ionospheric photoelectrons measured at geosynchronous orbit, MS thesis, Naval Postgraduate School, Monterey, CA, June 1993.

Lin, J., J. L. Horwitz, G. R. Wilson, C. W. Ho, and D. G. Brown, A semikinetic model for early stage plasmasphere refilling, 2. Effects of wave-particle interactions, *J. Geophys. Res., 97,* 1121-1134, 1992.

Lundquist, C. A., R. J. Naumann, and A. H. Weber, Directional flux densities and mirror-point distributions of trapped particles from satellite 1958e measurements, *J. Geophys. Res*., *67*, 4125-4133, 1962.

Olsen, R. C., Equatorially trapped plasma populations, *J. Geophys. Res*., *86*, 11235-11245, 1981.

Olsen, R. C., The density minimum at the earth's magnetic equator, *J. Geophys. Res., 97*, 1135-1150, 1992.

Olsen, R. C., C. R. Chappell, D. L. Gallagher, J. L. Green, D. A. Gurnett, The hidden ion population of the magnetosphere - Revisited, *J. Geophys. Res., 90,* 12121-12132, 1985.

Olsen, R. C. S. D. Shawhan, D. L. Gallagher, J. L. Green, and C. R. Chappell, Plasma observations at the earth's magnetic equator, *J. Geophys. Res., 92*, 2385-2407, 1987.

Persson, H., Electric field along a magnetic line of force in a low density plasma, *Phys. Fluids*, *6,* 1756-1759, 1963.

Persson, H., Electric field parallel to the magnetic field in a low density plasma, *Phys. Fluids, 9*, 1090-1098, 1966.

Scott, Lewis J., On the consequences of bi-Maxwellian distributions on parallel electric fields, M. S. thesis, Naval Postgraduate School, Monterey, CA, December 1991.

Singh, N., and D. G. Torr, Effects of ion temperature anisotropy on the interhemispheric plasma transport during plasmaspheric refilling, *Geophys. Res. Lett., 17*, 925-928, 1990.

Singh, N., and C. B. Chan, Effects of equatorially trapped ions on refilling of the plasmasphere, *J. Geophys. Res., 97*, 1167-1179, 1992.

Summers, D., and R. M. Thorne, A new tool for analyzing microinstabilities in space plasmas modeled by a generalized Lorentzian (kappa) Distribution, *J. Geophys. Res*., *97*, 16827-16832, 1992.

Swann, W. F. G., Application of Liouville's theorem to electron orbits in the Earth's magnetic field, *Phys. Rev., 44,* 224-227, 1933.

Vasyliunas, V., A survey of low-energy electrons in the evening sector of the magnetosphere with OGO 1 and OGO 3, *J. Geophys. Res., 73,* 2839-2884, 1968.

Whipple. E. C., The signature of parallel electric fields in a collisionless plasma, *J. Geophys. Res., 82*, 1525-1530, 1977.

Wrenn, G. L., J. F. E. Johnson, and J. J. Sojka, Stable 'pancake' distributions of low energy electrons in the plasma trough, *Nature, 279*, 512-514, 1979.

(Received September 22, 1992;
revised August 13, 1993;
accepted September 23, 1993.)